The USML-1 Wire Insulation Flammability Glovebox Experiment

Paul S. Greenberg/NASA Lewis Research Center
Kurt R. Sacksteder/NASA Lewis Research Center
Takashi Kashiwagi/National Institute of Standards and Technology

Introduction

Flame spreading tests have been conducted using thin fuels in microgravity where buoyant convection is suppressed. In spacecraft experiments[1] flames were ignited in quiescent atmospheres with an elevated oxygen content, demonstrating that diffusional mechanisms can be sufficient alone to sustain flame spreading. In ground-based facilities (ie. drop towers and parabolic aircraft) low-speed convection sustains flames at much lower concentrations of atmospheric oxygen[2,3,4,5] than in quiescent microgravity. Ground-based experiments are limited to very thin fuels (eg. tissue paper); practical fuels, which are thicker, require more test time than is available.

The Glovebox Facility provided for the USML-1 mission provided an opportunity to obtain flame spreading data for thicker fuel. Herein we report the results from the Wire Insulation Flammability (WIF) Experiment performed in the Glovebox Facility. This experiment explored the heating, ignition and burning of 0.65mm thick polyethylene wire insulation in low-speed flows in a reduced gravity environment. Four tests were conducted, two each in concurrent flow (WIF A and C) and opposed flow (WIF B and D), providing the first demonstration of flame spreading in controlled forced convection conducted in space.

Experiments

The Wire Insulation Flammability Experiment (WIF) was designed to observe: Joule heating of electrical wire in quiescent and low-speed forced-flows, and the ignition and spreading of a flame over the insulation of overheated electrical wire in very-low-speed flows. Four nearly-identical WIF test modules, designated WIF-A,B,C, and D were flown. Each module consisted of a miniature wind tunnel with flow provided by the glovebox air circulation system. A small spring-loaded anemometer indicated airflow velocity. A metal screen covering the exit port cooled combustion products and contained particulates released during combustion.

In each module a single polyethylene-insulated nichrome wire sample, 1.5 mm diameter, 110 mm long, was mounted parallel to the airflow direction. All tests were performed using Spacelab cabin air at approximately 21% oxygen at 1 atm. pressure. The polyethylene insulation was approximately 0.65 mm thick. Samples were ignited using Joule heated Kanthol wire wound around the sample end: near the flow-duct exit for opposed-flow burning or the entrance for concurrent flow. Each sample was instrumented with six type K thermocouples to measure wire, wire insulation and gas phase temperatures. Two windows were incorporated into the tunnel for photographic access. One window provided simultaneous video imaging of the sample and the thermocouple displays, the second window was used for 35 mm still photographs. Two 10 cc vacuum bottles with solenoid valves accompanied each test module to collect samples of off-gassing and combustion products. Two transmission electron microscope grids were attached to each exit screen to collect emitted particles.

The nominal test procedures consisted of heating the wire and insulation samples first in quiescent then in flowing air; thereafter the samples were ignited with the insulation at a temperature of approximately 373K. Video recordings were made of the entire sequence, motor-driven 35 mm still photographs were exposed during the flame spreading portion. Complementary flame spreading tests of duplicate but unheated WIF fuel samples were performed in normal gravity in ambient air. The fuel samples were oriented to burn either vertically upward, vertically downward, or horizontally.

Test Results and Discussion

Sample Preheating

Measurements of the sample preheating temperatures were obtained for each WIF module, each configured for different heating rates, in both quiescent and flowing conditions. The results, described in reference 6, show a similarity between quiescent microgravity heating in air and normal-gravity heating in a vacuum.

Ignition and Flame Spreading

Ignition of the insulation material was achieved in all four tests. The flames were quite bright and produced surprising amounts of soot. Soot and particles of condensed unburnt fuel vapor collected on the module exit screens. As the flames spread the fuel melted before vaporizing, and the molten fuel flowed into a quasi-spherical bulb moving with the flame.

Concurrent Flow Flame Spreading

WIF-A. The flame was quite bright, saturated the video imaging device, and appeared to pulsate. Analysis of the anemometer behavior indicates the pulsations could not be attributed to the forced flow but were intrinsic to the flame and attributed to bursting fuel vapor bubbles. Figure 1 is a monochrome reproduction of a 35mm color still photograph representing the concurrent flow flames. The flame was blue where the flow first met the flame, and became yellow further downstream. The tip of the flame was open, changing from yellow to a dark red, and soot visibly escaped from the flame, often in large thread-like structures.

As the flame propagated, the molten fuel accumulated, forming a growing, quasi-spherical bead 2-3 times the initial diameter of the insulation and not always symmetric with respect to the wire. Near the end of the test the gas-phase thermocouple, 1.5 mm from the virgin fuel surface, was occluded by the molten fuel. The surface of the fuel near the flame in WIF-A, as seen in the still photographs, was discolored and opaque, perhaps due to oxidative degradation of the polyethylene (this discoloration does not occur in normal gravity heating tests conducted in a nitrogen environment[7].) In a few of the still photographs, the opaque fuel surface appears to have been fractured or chipped, with an irregularly shaped gap in an otherwise uniformly brown surface. We speculate that a part of a rigid surface layer may have been ejected by a bursting vapor bubble.

WIF-C. In the third test, WIF-C, ignition was attempted without flow. A torroidal cloud of vapor or condensed pyrolysis products formed around the igniter and was rendered visible by the scattering of light emitted by the hot ignitor. The cloud ignited suddenly, and hot gas expansion was felt quickly by the anemometer 75 mm downstream. The flame burned weakly in quiescent air until 17 seconds after ignition when the flow was initiated. The flame immediately brightened, but ultimately failed to propagate. The downstream fuel ignited then extinguished under the combined effect, we speculate, of oxygen depletion by the upstream flame and retarded fuel vaporization suppressed by the layer of degraded polyethylene and soot on the fuel surface.

Opposed Flow Flame Spreading

WIF-B. The flames in all the WIF tests were quite bright. The more sensitive monochrome camera was selected before the flight to capture the expected dim flames, but could not accommodate both the bright flames and the dimmer temperature displays. In the second test, WIF-B, the crew member took the initiative, in real time, to adjust the video camera exposure to de-saturate the flame image. In so doing, the temperature displays were brought below the detection threshold of the video camera, but some imaging of the flame structure was recovered.

As in the concurrent flow test, the molten fuel accumulated into a bead under the flame, growing as the flame spread into the flow until reaching the steady size shown in fig. 2 in about 15-18 seconds. A dark surface layer, about 1-2 mm in length, appears near the flame stabilization point, again suggesting oxidative degradation. The still photographs show vapor bubbles in the molten fuel. Fluctuations in the flame and observed ejection of

small burning particles suggest the bursting of these bubbles. As the flame reached the end of the fuel sample, the flame shape altered, diverging downstream and more completely enveloping the molten fuel bead. As the stationary ball of fuel burned, more frequent flame perturbations occurred, suggesting higher vaporization rates. The fuel burned until it was completely consumed.

WIF-D. For the fourth test the monochrome video camera was replaced with a color camera. Real-time exposure adjustments provided balance between the flame and temperature display images. Acting on a suggestion of J.S. T'ien, the air flow was switched off after the flame reached the end of the sample. The flame quenched rapidly, leaving a nearly spherical fuel bead, 4-5 mm in diameter. This result provides a dramatic demonstration of the effect of low-speed flow on the flammability of materials in microgravity.

Normal-Gravity Flame Spreading

The normal-gravity experiments were characterized by significant dripping of the molten fuel away from the spreading flame. The mass of dripped fuel was as much as 1/2 of the total initial fuel mass. Flames in the normal gravity tests all had closed tips in contrast to the open downstream flame tips observed in all the WIF tests.

Flame Spread Rates and Lengths

The 35 mm photographic sequences provided better reproductions of the flame structure, particularly the blue leading edge of the flame (not visible in the video record). Thus while lacking the time resolution of the video record, the still photographs were used to obtain the flame spread rates of tests WIF-A,B, and D. Similar measurements were made from images of the normal gravity flames. The spread rate results are summarized in Table 1, where the normal gravity reflect average values from several tests.

Flame Spreading Direction	Flame Spread Rate	Fuel Burnout-Front Speed	Flame Length
Concurrent (WIF-A)	0.16 cm/sec	0.12 cm/sec	1.8-2.6 cm
Opposed (WIF-B)	0.070 cm/sec	-	1.8 cm
Opposed (WIF-D)	0.066 cm/sec	-	1.9 cm
Upward (1g)	-	0.13 cm/sec	-
Downward (1g)	0.24 cm/sec	0.18 cm/sec	
Horizontal (1g)	0.14 cm/sec	0.13 cm/sec	-

Table 1. Flame Spread Rates and Flame Lengths

Concurrent Flow. In concurrent flow, WIF-A, the visible downstream tip of the flame spread at an apparently steady 0.16 cm/sec; while the base of the flame (where the flame is stabilized and the fuel burnout occurs) spread at 0.12 cm/sec. The length of the flame grew slowly throughout the test at about 0.04 cm/sec. Thus even in the extended test time provided by the glovebox, concurrent flow flames clearly did not reach an equilibrium length. Though the possibility of steady propagation has been predicted for non-melting thin fuel[5], the WIF experiment did not provide a steady result.

The spreading of the flame tips in the normal-gravity upward burning tests were too rapid to measure with the 35mm still camera, ie. the flame length exceeded the length of the fuel sample within about three seconds. Propagation speeds of the fuel burnout front in the upward-burning test and the WIF-A concurrent-flow test were similar (0.13 and 0.12 cm/sec, respectively). Fuel consumption via melting and vaporization in the case of the

WIF-A experiment is quite different than the dripping observed in the upward burning experiment, however, so the similar burnout rates therefore appear to be coincidental.

Opposed Flow. The measured steady spread rates for the WIF-B and WIF-D, opposed-flow cases differ by only 6%, having values of 0.070 and 0.066 cm/sec respectively. The fuel in WIF-B was heated to 353K at ignition compared to 343K for WIF-D. Higher bulk-fuel temperatures have been correlated with increased flame spread rates in normal gravity.[8]

The normal-gravity downward burning flame spread rate of 0.24 cm/sec is much higher than the microgravity forced flow result. The open shape of the downstream flame tips in microgravity suggests under-ventilation. However, the overall equivalence ratio in the microgravity tests were very fuel-lean at about 1/45, and the bright leading edge of the flames suggest oxygen deprivation cannot account for the spread rate difference. In the several normal gravity tests, spread rates varied inversely with the measured fuel mass lost to dripping. Molten fuel in downward burning might enhance forward heat transfer (and the spread rate) if it flows ahead of the flame but does not drip completely from the fuel sample. Thermocapillary effects re-distribute molten fuel differently in microgravity, but more measurements would be needed to be quantitative. It is reasonable to infer that radiative losses, as in other microgravity tests,[1,5] contribute to lower microgravity spread rates; additional tests with varied flow velocities would help to clarify this issue.

Flame Temperatures

Temperature histories were obtained from the video record, and the data for the WIF-A and WIF-D experiments (Fig. 3). In WIF-A (concurrent flow) the first profile shows two gas-phase temperature peaks, representing first the flame tip and then the flame leading edge. The second profile shows the effect of the thermocouple being occluded by the molten fuel. The highest uncorrected temperature measured in the concurrent flow flame was 1333K. In normal gravity upward burning, the peak temperature of 1287K occurred near the flame bottom.

In WIF-D (opposed flow) the gas-phase temperature shows two peaks, represents first the flame leading edge then another peak near the trailing edge. The peak temperature in opposed flow was about 1273K. The temperature of the insulation rises rapidly to the pyrolysis temperature as the flame approaches, remains flat as the fuel vaporizes, then at burnout increases briefly to a high gas-phase temperature. Peak flame temperatures in normal gravity downward burning were found downstream, away from the leading edge and peaked at 1402K.

Soot and Particulate Production

Soot escaped from each WIF flame, most prolifically in the opposed-flow tests. Soot left the flame in strand-like structures approximately 10cm long and accumulated on the exit screens. In normal-gravity tests some soot also escapes and can be collected from the plume above the flames.

Transmission electron microscopic (TEM) analysis of the primary soot particles revealed mean diameters of 31 nanometers in the opposed-flow tests and 27 nanometers in concurrent flow, less than one standard deviation difference. Soot primaries collected in normal gravity showed mean diameters of 13 nanometers. The TEM analysis also showed transparent particles, 100-200 nm in diameter, on the exit screen of module WIF-C, perhaps condensed vapor from the quiescent ignition described above.

Many small bubbles were visible within the molten region, particularly in the opposed flow cases. Since the boiling temperatures of some polyethylene degradation products (products range from C_1 to C_{100} or higher)[7] are much less than the degradation temperature of polyethylene, when the degradation products are formed inside the sample they are immediately superheated and form bubbles. These bubbles grow by accumulation of degradation products through diffusion in the molten polyethylene. When they become sufficiently large and close to the surface, the pressure in the bubbles is sufficient to cause a sudden rupture, ejecting fragments of the molten polyethylene into the gas phase. The ejection of small burning polymer fragments were often observed during the flame spread process.

Conclusions

The WIF experiment results provide some introductory data for electrical wire insulation overheating and burning in a low-speed convecting environment, including flame size, structure, spread rates and temperatures. Some quantitative results were obtained: opposed flow flames were cooler, propagated slower and produced more soot than concurrent flow flames. These data are not sufficient to carry out extensive comparisons with normal gravity results mainly because of the limited number of tests, but provide quantitative information useful to the formulation of theoretical modeling and focussed additional tests.

Additionally, the WIF results provide stimulating demonstrations of some unique microgravity phenomenon. The behavior of the molten fuel, including the bead formation and bubble-bursting phenomena, the prodigious production and size of the soot agglomerates, the transient quenching in an abruptly-created quiescent environment, and the accumulation and ignition of vapor from overheated fuel are all phenomena seen first in these tests. Each of these phenomena have important implications in spacecraft fire scenarios: the quiescent quenching demonstration has been used to convince the STS program to adopt ventilation flow cutoff as a fire fighting procedure.

References

1.) Bhattacharjee, S., Altenkirch, R.A., and Sacksteder, K.R., "Implications of Spread Rate and Temperature Measurements in Flame Spread Over a Thin Fuel in a Quiescent, Microgravity, Space-Based Environment," *Combust. Sci. Tech.*, 91, pp.225-242, (1993).

2.) Olson, S.L., Ferkul, P.V., and T'ien J.S., "Near-Limit Flame Spread Over a Thin Solid Fuel in Microgravity," *Twenty-Second Symposium (International) on Combustion*, the Combustion Institute, pp. 1213-1222, (1988).

3.) Olson, S.L., "Mechanisms of Microgravity Flame Spread Over a Thin Solid Fuel: Oxygen and Opposed Flow Effects," *Combust. Sci. and Tech.*, 76, pp. 233-249, (1991).

4.) Sacksteder, K.R., and T'ien, J.S., "Buoyant Downward Diffusion Flame Spread and Extinction in Partial-Gravity Accelerations," presented at the *Twenty-Fifth Symposium (International) on Combustion*, The Combustion Institute, in press (1995).

5.) Grayson, G.D., Sacksteder, K.R., Ferkul, P.V., and T'ien, J.S., "Flame Spreading Over a Thin Solid in Low Speed Concurrent Flow: Drop Tower Experimental Results and Comparison with Theory," *Microgravity Sci. Technol.*, Vol.7, no.2, (1994).

6.) Greenberg, P.S., Sacksteder, K.R., Kashawagi, T., "Wire Insulation Flammability Experiment: USML-1 One Year Post Mission Summary," *Proceedings of the Joint Launch Plus One Year Science Review of USML-1 and USMP-1 with the Microgravity Measurement Group*, NASA CP 3272, Vol.2, (1994).

7.) Madorski, S.L., *Thermal Degradation of Organic Polymers*, John Wiley and Sons, Chapter 4, 1964.

8.) Borgeson, R.A., and T'ien, J.S., "Modelling the Fuel Temperature Effect on Flame Spread Limits in Opposed Flow," *Combust. Sci. and Tech.*, 32, pp. 125-136, (1983).

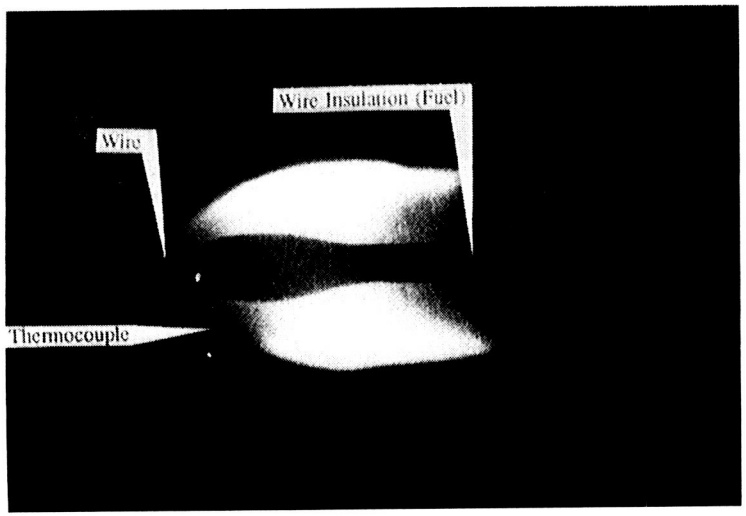

Figure 1. WIF A, Concurrent-Flow Flame

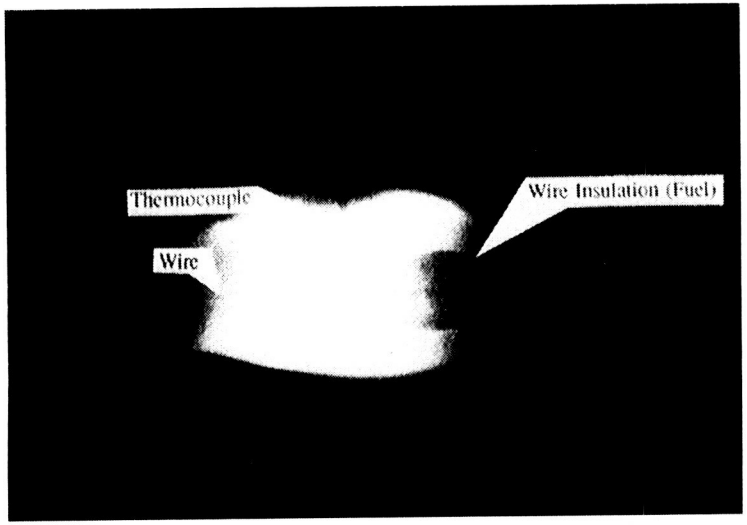

Figure 2. WIF B, Opposed-Flow Flame

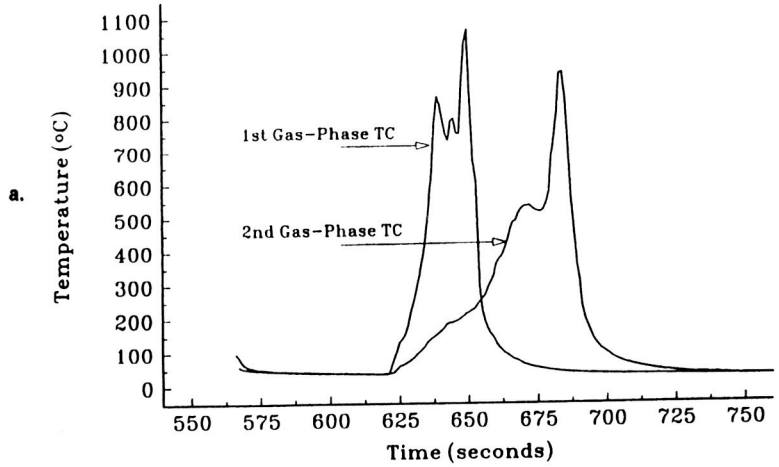

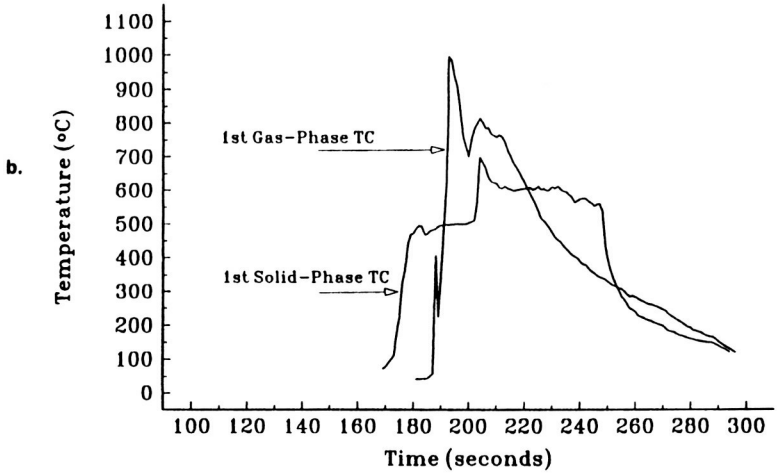

Figure 3. Temperature Measurements: a) Concurrent Flow and, b) Opposed Flow